Performance optimization of a Two-Stroke supercharged diesel engine for aircraft propulsion

Antonio Paolo Carlucci*, Antonio Ficarella, Gianluca Trullo

Antonio Paolo Carlucci, PhD, Assistant Professor
University of Salento
Department of Engineering for Innovation
Via per Monteroni - 73100 Lecce, Italy

Antonio Ficarella, PhD, Full Professor
University of Salento
Department of Engineering for Innovation
Via per Monteroni - 73100 Lecce, Italy

Gianluca Trullo, PhD Student
University of Salento
Department of Engineering for Innovation
Via per Monteroni - 73100 Lecce, Italy

*Corresponding Author:
Antonio Paolo Carlucci
Assistant Professor - Systems for Energy and Environment
University of Salento - Dept. Engineering for Innovation (CREA)
via per Monteroni - 73100 LECCE
tel. +39 0832 297751; mob. +39 340 6925653
fax.+39 0832 297777
email: paolo.carlucci@unisalento.it

Abstract

In Two-Stroke engines, the cylinder filling efficiency is antithetical to the cylinder scavenging efficiency; moreover, both of them are influenced by geometric and thermodynamic parameters characterizing the design and operation of both the engine and the related supercharging system. Aim of this work is to provide several guidelines about the definition of design and operation parameters for a Two-Stroke two banks Uniflow diesel engine, supercharged with two sequential turbochargers and an aftercooler per bank, with the goal of either increasing the engine brake power at take-off or decreasing the engine fuel consumption in cruise conditions. The engine has been modeled with a 0D/1D modeling approach. Then, the model capability in describing the effect of several parameters on engine performance has been assessed comparing the results of 3D simulations with those of 0D/1D model. The validated 0D/1D model has been used to simulate the engine behavior varying several design and operation engine parameters (exhaust valves opening and closing angles and maximum valve lift, scavenging ports opening angle, distance between bottom edge of the scavenging ports and bottom dead center, area of the single scavenging port and number of ports, engine volumetric compression ratio, low and high pressure compressor pressure ratios, air/fuel ratio) on a wide range of possible values. The parameters most influencing the engine performance are then recognized and their effect on engine thermodynamic behavior is discussed. Finally, the system configurations leading to best engine power at sea level and lowest fuel consumption in cruise conditions – respectively +42% and -7% with respect to baseline – have been determined implementing a multicriteria optimization procedure.

Keywords

Two-Stroke diesel engine, aircraft propulsion, breathing system, Multiobjective optimization, Engine supercharging, Uniflow scavenging

1. Introduction

Due to increasingly stringent request for higher performance and lower fuel consumption, the definition of supercharging system in reciprocating engines for aircraft propulsion is a crucial task [1-3]. In Two-Stroke engines, particular care must be addressed in designing the breathing system in order to obtain a good scavenging process, whose effectiveness is quantified by both the Scavenging Efficiency (SE) and Trapping Efficiency (TE).

Many parameters affect the scavenging process. Ravi and Marathe in [4] conducted a numerical analysis on the effect of size, opening and closing timings of both scavenging ports and exhaust valves on the flow field established in the cylinder of an Uniflow Two-Stroke engine. The analysis, conducted in transitory conditions, revealed that: 1) a larger size, an earlier opening and a delayed closure of the inlet ports lead to better gas exchange process; 2) the earlier the exhaust valve closes, higher is TE but lower is SE; moreover, properly choosing the exhaust valve closing angle, it is possible to obtain best scavenging process or minimal fresh charge loss.

The effects of inlet duct length, geometric port swirl angle, and number of ports on swirl generating capability in the cylinder of an Uniflow Two-Stroke engine have been explored by Ravi and Marathe in [5]. It was proven that the pressure value at the inlet and exhaust have a global effect on the scavenging process; in particular, the higher the pressure drop between inlet and exhaust, the better is SE, but, at the same time, TE deteriorates.

Fleck and Cartwright in [6] measured the coefficients of discharge in high performance Two-Stroke engines varying different engine architectures. Modifying the inlet and exhaust ports section, it was found that the discharge coefficient variation is caused by duct geometry only in the case of inlet ports, while it is function of the pressure ratio as well in the case of the exhaust system.

Laser Doppler Velocimetry measurements allowed, as reported for example in [7] and [8], to characterize the velocity field at the exit of intake ports of a Two-Stroke engine. This helped assessing the goodness of different intake geometries in improving SE.

More recently, Kinoshita and Motoyama in [9] proposed a model for the scavenging process of a Loop scavenged Two-Stroke engine, function of shape, section and tangential angle of inlet ports, based on the experimental observations using a three-dimensional anemometric-tester. As a result, with the goal of optimizing the engine performance, it is necessary: 1) to direct the airflow coming from the main transfer port toward the center of the bore and 2) the inner vent radius of the main transfer duct to assume a relatively large value.

The optimization of the scavenging system has been also pursued using CFD approach. Mattarelli et al. in [10] reports 3D models of several architectures and different scavenging configurations including different bowl shapes for Two-Stroke compression ignition engines. According to the different proposed layouts, SE, TE, air purity, fresh air concentration, velocity vector magnitude and mean effective pressure have been calculated at different engine speed for both Loop and Uniflow scavenging systems. Furthermore, a comparison between the two different scavenging models has been run using KIVA software analyzing several engine output parameters. The attained output parameters revealed that the well-known performance gap between Loop and Uniflow scavenged engine could be slightly reduced by a 3D CFD design support; furthermore, considering the same Two-Stroke engine (either for automotive or aircraft propulsion), scavenged

with one of the previous systems, presents better performance than the related 4 strokes engine and, at the same time, lower emissions.

Leep et al. in [11] report the simulation results of the scavenging process, taking place in a three-cylinder engine, obtained coupling a 3D CFD and a 0D/1D models. Simulations were run over the whole engine characteristic map; investigating the outputs obtained in different operating conditions, it was revealed that the scavenging process becomes hard to manage and then detrimental when the engine speed increases. Furthermore, the 3D study demonstrated that the flow field vectors inversion weakly influence the process, but the orientation of inlet ports is able to modify the flow velocity field changing the phenomena associated to fuel injection and combustion. Considering the interactions taking place in a multi-cylinder engine, it has been determined that, at high engine speed, the final combustion pressure reaches a higher value but the scavenging process is further penalized.

In [12] the effect of several design parameters of a Two-Stroke Uniflow engine on the swirl generated into the combustion chamber, and then the quality of the scavenging process, was studied using ARIS 3D code. The Authors highlighted that the swirl level increases if the length of the inlet duct increases as long as it reach a maximum; from that point on, pressure losses become relevant. Equally, increasing the swirl angle as well as the number of ports generates high swirl level producing, though, high pressure losses.

In order to obtain the best engine performance, all the parameters affecting its behavior must be carefully tuned [13-15]. Multi-objective optimization based on genetic algorithms are often used to support the tuning process of a multivariable system drastically reducing the required time [16].

Aim of this work is to provide several guidelines about the definition of design and operation parameters for a Two-Stroke two banks Uniflow diesel engine, supercharged with two sequential

turbochargers and an aftercooler per bank, with the goal of either increasing the engine output power at take-off or decreasing the engine fuel consumption in cruise conditions. The engine has been modeled with a 0D/1D modeling approach. Then, the model capability in describing the effect of several parameters on engine performance has been assessed comparing the results of 3D simulations with those provided by 0D/1D model. The validated 0D/1D model has been used to simulate the engine behavior varying many design and thermodynamic parameters. Then, the effect of most influential parameters on engine brake power (P_b) at Sea Level (SL) and specific fuel consumption (BSFC) in cruise condition (CC, corresponding to an altitude equal to 10680m) has been analyzed. Finally, the configurations optimizing the aforementioned engine performance have been determined.

2. Engine model

The engine analyzed in the present work is a Two-Stroke diesel engine for aircraft propulsion, composed by six cylinders arranged in two independent banks. The scavenging system is Uniflow, with 14 inlet ports and 2 exhaust valves per cylinder. The supercharging system consists of two turbochargers and one aftercooler per bank. This configuration has been selected since it proved to be the only one, among the configurations analyzed in [1], able to guarantee the target engine brake power at different altitudes with the minimum fuel consumption. The engine main specifications are reported in Table 1, while a general scheme of the engine layout is shown in Figure 1.

Table 1 – Engine main specifications

Cycle	Two-Stroke Diesel Uniflow
Bore/Stroke	1

Compression ratio	17.2:1
Injection system	common rail
Engine speed	2000 rpm
Inlet ports opening/closing angles	115 CAD ATDC/245 CAD ATDC
Exhaust valves opening/closing angles	80 CAD ATDC/250 CAD ATDC

Figure 1 – Schematic representation of the engine (single bank)

The software used for modeling the engine is AVL Boost v2011.2, characterized by a 0D/1D approach. This approach has been preferred since it is functional for obtaining meaningful results about the behavior of the whole engine with a not excessive computational time. More details about the software can be found in [17], while the model description and calibration are illustrated in [1]. Regarding the scavenging model, the one used in this paper is the model suggested by Blair [18] representing an intermediate approach between the *perfect mixing* and the *perfect displacement* models:

$$SE = 1 - \exp(4.35 + 1.36DR - 0.22DR^2) \quad \text{(eq. 1)}$$

where *DR* is the Delivery Ratio, defined as the ratio between the mass of fresh charge entering the cylinder during the scavenging process and the air mass at ambient conditions necessary to fill the cylinder.

3. Optimization procedure of the engine breathing system

The architecture with two turbochargers and one aftercooler per bank was further investigated, seeking for the design trends for the breathing system optimizing the engine performance. A multiobjective optimization procedure was chosen, finalized to the determination of the engine parameters maximizing P_b at SL and BSFC in CC. During the optimization process, several parameters have been varied, like: Exhaust Valves Opening (EVO) and Closing (EVC) angles and maximum Valve lift (HEV), Inlet/scavenging Ports Opening angle (IPO), distance between bottom edge of the scavenging ports and bottom dead center (HBI), area of the single scavenging port (A) and number of ports (n), engine volumetric Compression Ratio (CR), low (PR_{LP}) and high (PR_{HP}) pressure compressor pressure ratios, Air/Fuel Ratio (AFR). These parameters have been varied on discrete levels in an acceptable range of values.

However, before running the optimization process, the suitability of the 0D/1D engine model in predicting the effect of several among the varied parameters on TE and SE, and consequently on P_b and BSFC, has been verified. This validation process was necessary since AVL Boost models the strictly 3D fluid-dynamics phenomena using coefficients [17]; therefore, its capability in describing the effect of the varied parameters on the engine performance was not obvious.

3.1 Validation of 0D/1D model

In order to verify the capability of the 0D/1D numerical model generated in AVL Boost in modeling the effect of the varied parameters, the scavenging processes have been simulated with Ansys Fluent CFD 3D simulation software. The validation of the 0D/1D model has been done varying on two levels some of the parameters varied during the optimization procedure, and then comparing the results, in terms of SE and TE, obtained with the two models. The validation has been done on geometric parameters showing a significant effect on SE and TE (as it will be seen later). In

particular, these variables have been: “n” and A at intake side; EVO and EVC at the exhaust side. The parameters values for each 3D simulation are reported in Table 2:

Table 2 – 3D simulations

Simulation	Description	EVO [CAD ATDC]	EVC [CAD ATDC]	n [-]	A [mm^2]
1	Default	73	233	12	225
2	EVO Variation	**98**	233	12	225
3	EVC Variation	73	**258**	12	225
4	n Variation	73	233	**16**	225
5	A Variation	73	233	12	**275**

The two values for each parameter have been chosen in order to cover as much as possible the variation range that will be set for the optimization procedure (see Table 4). In this way, it was possible to study the effect of the variation of each parameter at a time, with only five simulations. The scavenging process, purely transient, was simulated using dynamic mesh in order to properly describe the movement of the piston - obstructing the scavenging ports - and of the exhaust valves. The different kinds of mesh used to create the dynamic model are indicated in Figure 2:

Figure 2 – Mesh zones

As reported in Figure 2, it is possible to recognize three different kinds of mesh: fixed, i.e. not subjected to movements; rigid body, i.e. moving in the space without changing its former shape (rigid movement); layering, i.e. moving and changing its shape (and volume). The latter kind of

mesh is used to model the regions surrounding the valves (indicated in Figure 2 with 2, 3 and 4) and piston (indicated with 6); in particular, having to allow either straight motion and collapsing of the unused layers (dynamic layering), cubic or hexahedral elements have been used, as shown in Figure 3.

Figure 3 – Cells shape

The real geometry of the engine plenum, from which the air enters the cylinder through the scavenging ports, has been replaced with another plenum having an annular section around the cylinder liner (see Figure 4) and an overall volume doubled respect to the original plenum. This choice was made in order to make negligible the initial air velocity and to simplify the mesh and so shorten the computational time. The boundary conditions at cylinder intake and exhaust sides have been imposed based on the results obtained with AVL Boost simulations at SL. In detail, the dynamic pressure in the plenum and at exhaust during scavenging phase have been imposed equal to its average value - based on 0D/1D simulations - in the range 80-250 CAD ATDC for the plenum while in the range 150-250 CAD ATDC at the exhaust, so excluding the initial scavenging phase strongly influenced by a transonic flux through the exhaust valves. In Figure 4 the boundary sections at intake and exhaust are highlighted. Moreover, initial values – values related to starting time of the simulation - in terms of pressure, temperature and molar fraction in the plenum, into the cylinder and at the exhaust have been calculated running the simulation with 0D/1D model using the same values for the parameters reported in Table 2. Another condition imposed for simulations with 0D/1D model was related to the instant difference between inlet and exhaust pressure difference; in particular, it was desired to have comparable values for all the cases

reported in Table 2. Table 3 lists the data setting related to 3D boundary conditions for all the different run simulations, in terms of parameters values.

Figure 4 – Boundary sections at cylinder inlet and exhaust for 3D simulations

Table 3 - Boundary and initial conditions for 3D simulations calculated via 0D/1D model

Simulation #		**1**	**2**	**3**	**4**	**5**
Simulation Range	[CAD ATDC]	**73-233**	98-230	73-258	73-233	73-233
p_cylinder @ *EVO*	[barg]	**21.8**	11.5	21.1	23.5	21.9
p_plenum_mean @ *EVO*	[barg]	**17.3**	18.7	17.0	16.9	17.2
p_exhaust_mean @ *EVO*	[barg]	**13.2**	15.0	12.9	12.7	13.3
Delta_p_IN-OUT_cyl	[bar]	**0.411**	0.365	0.410	0.420	0.388
T_cylinder @ *EVO*	[K]	**1679**	1466	1731	1728	1683
T_plenum @ *EVO*	[K]	**331**	335	329	326	331
T_exhaust @ *EVO*	[K]	**511**	636	371	404	510
air_fraction_plenum @ *EVO*	[-]	**1.00**	1.00	1.00	1.00	1.00
air_fraction_cylinder @ *EVO*	[-]	**0.00**	0.00	0.00	0.00	0.00
air_fraction_exhaust @ *EVO*	[-]	**0.80**	0.60	0.97	0.94	0.81

Total mass flow rates at inlet, total mass and air mass flow (the so called short-circuit air, i.e. the air entering the cylinder flowing directly towards the exhaust) rates at exhaust predicted with 0D/1D and 3D models are compared respectively in Figs 5a, 5b and 5c. It can be stated that the main filling and emptying phenomena are generally concordantly predicted. A more detailed analysis of Figure 5a reveals that two backflows, both penalizing the scavenging process, are simulated by 3D model but not by 0D/1D model: the first, between 115 and 130 CAD ATDC, during which a part of the exhaust gases flow back in the plenum; the second, during the final phase of the scavenging process between 220 and 245 CAD ATDC, in which part of the fresh charge flows back again in the plenum. Results reported in Figure 5c, on the other hand, demonstrate that both

models predict a positive value of the air mass flow rate during almost all the scavenging phase – although not perfectly phased – determining a lower value for TE.

Figure 5 – Instantaneous and cumulative values for cylinder inlet, exhaust and short-circuit mass flow rates for simulation 1 (default)

The results of the simulations representative of the conditions listed in Table 2 run with 0D/1D and 3D codes are compared, in terms of SE and TE, respectively in Figure 6a and 6b, as percentage variation with respect to the default conditions (simulation 1).

Figure 6 – Relative SE and TE variation referred to the default conditions (simulation 1)

Analyzing Figure 6, it is possible to notice a good accordance in the trends related to the variation parameters obtained with 0D/1D and 3D codes. In particular:

- Increasing EVO, and then delaying exhaust valve opening, determines the increase of TE and the reduction of SE; this effect – consistent with results reported in [4] – is justified taking into account that, delaying the EVO, the exhaust blowdown is weakened, and so the scavenging induced by the exhaust gas inertia effect;

- Increasing either EVC, “n” or A determines a reduction of TE, in agreement with results reported in [4]; in detail, A exhibits a negligible effect, while EVC and “n” significantly influence TE. Opposite behavior is shown by the SE. Delaying EVC, in fact, allows more fresh air to be short-circuited through the exhaust valves; increasing “n”, on the other hand, contributes to better scavenge the cylinder, at the expenses of TE.

Since the main goal of this work is to provide guidelines concerning the design of the breathing system and not their quantitative values, the predictive capability of 0D/1D code can be considered acceptable for further considerations.

3.2 Input parameters for the optimization process

Two-Stroke engine performance, as previously said, are significantly affected by the breathing system because of its effect on SE and TE. For this reason, a multiobjective optimization process, oriented to obtain a fluid dynamic design trend for the engine breathing system as a whole, has been implemented and run in ModeFrontier software [19]. During this process, the aforementioned parameters have been varied. In Table 4 the parameters varied during the optimization procedure are listed, specifying, for each of them, the actual value, the lower and upper bounds, the central value and the variation step.

Table 4 - Design and thermodynamic input parameters defining the engine breathing system

Acronym	Unit	Actual Value	Lower Bound	Upper Bound	Central Value	Step
CR	[-]	17.2	13	18	15.5	0.2
EVO	[DCA ATDC]	80	60	110	85	5
EVC	[DCA ATDC]	250	220	270	245	5
HEV	[mm]	12	8	14	11	0,5
IPO	[DCA ATDC]	115	100	130	115	2.5
A	[mm^2]	265	200	300	250	5
“n”	[-]	14	10	19	14.5	1
HBI	[mm]	2.5	1	3	2	0.25
AFR	[-]	20	17	27	22	0.5
PR_{HP} @ SL	[-]	1.7	1.2	2.2	1.7	0.05
PR_{LP} @ SL	[-]	1.75	1.2	2.2	1.7	0.05
PR_{HP} @ CC	[-]	2.3	2.2	3.4	2.8	0.05
PR_{LP} @ CC	[-]	3	2.2	3.4	2.8	0.05

3.3 Optimization procedure

Goal of the multiobjective optimization was to study the effect of the aforementioned parameters on P_b at SL and BSFC at CC. The engine model was run varying all the input parameters on the range of allowed values, as well as the ambient conditions (SL and CC). The constraints imposed in order to consider a design as acceptable were: 1) maximum in-cylinder pressure not higher than 150 bar; 2) maximum temperature at the aftercooler outlet not higher than 473.15 K; 3) maximum exchanged heat power in the aftercooler not higher than 40 kW. The ModeFrontier Design of Experiments (DoE) generated 30 random starting solutions; for each of them, the genetic algorithm MOGA II [19] generated 70 combinations. All the 2100 resulting configurations defined the Pareto front.

For this purpose, the workflow shown in Figure 7 has been implemented. In this flowchart, it is possible to recognize several groups of operational blocks:

Figure 7 – ModeFrontier Multiobjective Optimization workflow

- *Input variables*: some of them, such are EVO and EVC, HEV, IPO A HBI and “n”, were manipulated in Matlab to generate the temporal evolution of scavenging port and exhaust valves flow sections, required as input in AVL Boost;
- *ModeFrontier Operational Blocks*: these two blocks create the population of designs to be optimized (DoE block) and run the genetic algorithm in order to find the desired solutions (Scheduler MOGA II – Multi-Objective Genetic Algorithm II);
- *External Script Blocks*: these two blocks allow ModeFrontier to run the analysis using the array of input parameters generated by the DoE;

- *Output Variables*: they represent the values to be optimized and, in addition, the thermodynamic constraints to be fulfilled; it is possible to recognize P_b and BSFC (goal parameters), the maximum in-cylinder pressure (pmax), the thermal power exchanged in the aftercooler (Wic) and the airflow temperature downstream the aftercooler (Tic);
- *Constraints*: they are the numerical representation of the limitations on pmax, Wic and Tic;
- *Goals*: they represent the optimization functions necessary to be implemented to reach the desired goals.

The result of this optimization process is the determination of every single point that will compose the well-known Pareto Front [16].

4 Data analysis and discussion of results

Pareto front is composed by a series of optimum solutions defined as “non-dominated”. This means that each solution composing the Pareto front is the best achievable solution for the optimization problem using a specific set of input parameters [16]. Referring to the proposed optimization analysis, using a statistical approach to interpret the obtained results and more specifically to investigate the effect that every input variable has on the output values (P_b and BSFC) has been considered essential, given the significant amount of input variables and the high discretization for each of them. To reach this goal, the t-Student test approach was selected to manage all the available data. Then, the Effect Size (ES) and the Significance (S) were used as meaningful statistical results. ES, as reported by Ferguson [20], estimates the correlation magnitude between two or more variables. ES was estimated as described in [21] and [22]. The Significance value S, on the other hand, evaluates the statistical goodness of the previous analysis; low value of S means that the computed ES value has high probability to be true.

In Table 5 the statistical parameters ES and S are listed, relating each input parameter with each goal function.

Table 5 - Statistic parameters ES and S associated to each input

Goal Function	Statistical Parameter	Input Parameters										
		CR	AFR	EVC	EVO	HEV	IPO	A	"n"	HBI	PR_{LP}	PR_{HP}
P_b @SL	ES	11.6	-53.6	16.39	3.32	-2.28	-1.53	1.9	-7.5	-24.9	32.26	49.76
	S	0	0	0	0	0.04	0	0.052	0	0	0	0
BSFC @CC	ES	-18.7	35.15	-15.4	-13.8	0.88	-16.8	19.84	-12.7	- 9,36	-31.6	-34.1
	S	0	0	0	0	0.22	0	0	0	0	0	0

The analysis of the determined values have to follow different paths depending on the parameter considered; while for S a value as low as possible is desired, for ES it is difficult to decide whether that value is significant or not. Since an absolute reference value is not available, the analysis will focus on the relative comparisons between the computed values.

4.1 Engine brake power maximization

From Table 5 it can be noticed that AFR, PR_{HP}, PR_{LP}, assume the highest ES values. As expected, decreasing AFR determines a higher power available to turbines and then a higher air mass flow delivered by the compressors to the cylinders; this, in turn, allows to burn more fuel, so increasing the cylinder pressure and therefore P_b. On the other hand, increasing PR_{HP} and PR_{LP} determines a higher amount of air trapped into the cylinder, therefore more fuel burned and higher P_b; the upper limits for both PR are determined by the constrain imposed on the maximum cylinder pressure.

A lower value of ES is then assumed by HBI. In Figure 8 the mass flows at cylinder inlet and outlet are reported for two extremes values (low=1mm; high=3mm) of HBI. It is visible that a low HBI determines a slightly higher mass flow rate flowing at both the intake and exhaust. This can be due to the fact that a low HBI value determines lower intake flow areas, as visible in Figure 8, and then higher inlet velocity, thus helping the scavenging process. The final result is a higher air mass trapped into the cylinder and consequently a higher P_b.

Figure 8 – Comparison between cylinder inlet and outlet mass flow rates and effective flow areas related to low (=1mm) and high (=3mm) value of HBI

Referring back to Table 5, (positive) values of ES lower than HBI are assumed by EVC and CR. Concerning EVC, it is immediate to observe that, changing EVC, the scavenging process also changes because of the higher/lower available time for gas exchange. Therefore, a delayed EVC determines a higher P_b because the longer the exhaust valve is open, the better is the scavenging process. On the other hand, an advanced EVC generates a worse scavenging efficiency and consequently a lower P_b. Concerning CR, when this parameter assumes high values, the in-cylinder pressure reaches high values determining high indicated work and consequently high P_b, without penalization on the scavenging process.

A further lower - negative - value of ES is assumed by “n”, i.e. the number of inlet ports. In Figure 9 the mass flow rates at cylinder inlet and outlet are reported for two extremes values (low=10; high=19) of n. The higher value of mass flow at inlet obtained with a low value of “n” can be due to the higher inlet velocity, leading to a better cylinder scavenging, a bigger amount of trapped air and therefore a higher P_b.

Figure 9 – Comparison between cylinder inlet and outlet mass flow rates and effective flow areas related to low (=10) and high (=19) value of "n"

The remaining parameters EVO, HEV, A and IPO are not discussed since characterized by a ES value very low compared to those characterizing the other parameters; moreover, the related S values for some of them are not very low, therefore the probability for ES values to be true is low.

4.2 Engine Specific Fuel Consumption Minimization

In cruise condition too, the most influencing parameters, according to ES values reported in Table 5, are AFR, PR_{HP}, PR_{LP}. It is possible to notice also that the sign of almost all the ES values is opposite to the ones related to P_b.

Considering AFR and its ES, it is obvious that, when it increases, BSFC has the same behavior. This is explainable considering that, when AFR increases, the amount of fuel feeding the engine is lower. A low quantity of fuel generates lower exhaust gases energy exploitable by the turbines which, in turn, transfer less power to the compressors. All these phenomena result in lower compressor pressure ratios and engine efficiency, therefore a higher BSFC.

After AFR, the most significant parameters are PR_{HP} and PR_{LP}; according to the sign of the ES, if PR_{HP} and/or PR_{LP} increase, BSFC decreases. In fact, in these conditions the engine traps more air mass that allows to burn a greater amount of fuel; in this way, more thermal power is available for the turbines and then for the compressors. This determines an increase in the conversion efficiency, so a lower BSFC.

Analyzing the remaining parameters in Table 5, the following lower ES value is related to A, the single port section. According to the sign of the relative ES, the higher is the section of the single port, the higher is BSFC. This can be explained considering how SE is affected by the variation of this parameter: the smaller the section of the single port, the higher the air velocity through it. This generates higher value of SE because the higher air velocity pushes out a larger amount of residual gas and reduces, at the same time, short-circuit air flow that worsen the overall efficiency. That aspect is quite clear observing the mass flow behaviour as a function of the crank angle plotted in Figure 10. The plotted curves are obtained with two extreme values of A: low (=200mm^2) and high (=300mm^2). Curves related to the lower value of A show higher mass flow rates right after IPO – because of the higher air velocity – determining a higher SE; later on, the mass flow rate related to the higher value of A increases and overcomes the lower mass curve because of the bigger flow area.

Figure 10 – Comparison between cylinder inlet and outlet mass flow rates and effective flow areas related to low (=200mm^2) and high (=300mm^2) value of A

The next parameter with lower ES value is CR; the sign of ES is negative and then, when CR increases, BSFC, as well known, decreases.

The following parameter with lower (negative) ES is IPO, so, increasing (delaying) IPO, it is possible to reduce BSFC. Delaying IPO, in fact, determines a better scavenging process; in this way, the overall efficiency increases and BSFC decreases. The lower is the IPO value, the longer is the time interval to scavenge the cylinder, increasing the short-circuit mass flow rate and so reducing the efficiency. In order to prove what stated, the mass flow rate at cylinder inlet and outlet with low (=100 CAD) and high (IPO=130 CAD) IPO values are plotted in Figure 11. The curve related to the

lower IPO shows a lower peak mass flow rate at inlet and a wider scavenging time interval determining a lower air velocity and then a worse scavenging process.

Figure 11 – Comparison between cylinder inlet and outlet mass flow rates and effective flow areas related to low (=100 CAD) and high (=130 CAD) value of IPO

Finally, considering EVO and EVC, opening and closing exhaust valves angles, both have negative values and then BSFC decreases when they are delayed. This is determined by a scavenging process characterized by a weaker exhaust blowdown caused by a lower pressure ratio through the valves (delayed EVO) leading to a higher TE but to a lower SE, and by a longer, and therefore more effective, scavenging process (delayed EVC).

The remaining parameters characterized by lower ES value and/or higher S value are not analyzed.

5. Multi criteria decision making

The described optimization process has generated a high number of solutions that, due to the property of the algorithm, compose the Pareto front. The final goal of the analysis might be to find the values (geometrical and thermodynamic) redesigning the breathing system as a whole; for this reason, among all the generated solutions, the one defining the configuration maximizing P_b at SL and the one minimizing BSFC in CC are highlighted. Table 6 summarizes the two different optimal parameters sets for the aforementioned operating conditions, with the related values of TE and SE. Specifically, both P_b and BSFC are reported in % of the relative original values. Finally, Figure 12 depicts the two Pareto fronts (one for each flight level).

Table 6 – Parameters values for maximum P_b (SL) and minimum BSFC (CC)

Flight level	P_b [%]	BSFC	A	AFR	CR	EVC	EVO	HBI	IPO	HEV	PR_{LP}	PR_{HP}	n	TE	SE
SL	142.34	99.75	240	17	16	270	110	1	115	10.5	1.7	2.1	10	0.92	0.69
CC	120.77	92.92	225	18.5	18	240	95	2	122.5	11	2.7	2.7	17	0.89	0.75

Figure 12 – Pareto front SL (a) and CC (b) optimization processes; red points represent maximum P_b case (A) and minimum BSFC case (B)

In detail, the results obtained for the maximization of P_b indicate that AFR, "n" and HBI must assume low values in the range allowed during the optimization procedure, as expected considering their effect on P_b (Table 5). For the same reason, EVC, EVO, PR_{LP} and PR_{HP}, must assume high values in the range allowed during the optimization procedure, the last two eventually limited by the limitation on the maximum cylinder pressure. The last four variables CR, A, IPO and HEV – the last three characterized by a weak effect on P_b as reported in Table 5 – assume intermediate values in order to achieve the best TE and so burn the maximum amount of fuel, having opposite effects on P_b as reported in Table 5.

Concerning BSFC minimization, the results obtained indicate that AFR and A must assume low values in the range allowed during the optimization procedure, as expected considering their effect on P_b (Table 5). For the same reason, CR, IPO and "n" must assume high values in the range allowed during the optimization procedure. The last variables EVC, EVO, HBI, PR_{LP}, PR_{HP} and HEV – the last one characterized by a weak effect on BSFC as reported in Table 5 – assume intermediate values in order to achieve the best compromise between TE and SE.

6. Conclusions

Aim of this work is to provide guidelines for the optimization of the performance of a Two-Stroke Uniflow diesel engine for aircraft propulsion by properly designing the breathing system. The supercharging system of the engine is characterized by two turbochargers and an aftercooler per bank. A 0D/1D numerical model of the engine has been created with AVL Boost software. Furthermore, its capability in modeling the effect of several design parameters has been verified comparing the results provided with the 0D/1D model with those provided by a 3D model run in Ansys Fluent.

Then, a multiobjective optimization process has been implemented and run in ModeFrontier software, during which several design and thermodynamic parameters have been varied on a range of allowed values. Goal of this process was to maximize engine output power at take-off and to minimize specific fuel consumption in cruise conditions. The main findings of the optimization procedure are summarized in the following:

- Air/Fuel ratio, low and high pressure compressor pressure ratios were the most influent parameters affecting engine output power and specific fuel consumption;
- In take-off conditions, also the distance between bottom edge of the scavenging ports and bottom dead center, the exhaust valve closing angle, the engine volumetric compression ratio and the number of scavenging ports resulted to be significant in determining the engine output power; the optimized configuration allowed to reach a very high value of the trapping efficiency, and so burn the maximum amount of fuel;
- In cruise conditions, the area of the single scavenging port, the engine volumetric compression ratio, the inlet port opening angles together with the exhaust valves opening and closing angles resulted to be significant in determining the engine specific fuel

consumption; the optimized configuration allowed to achieve the best compromise between trapping and scavenging efficiency.

7. Acknowledgments

The Authors would like to acknowledge Dr. Alessandro Renna for his assistance in engine modeling activities.

8. Bibliography

[1] Carlucci AP, Ficarella A, Laforgia D, Renna A. Supercharging system behaviour for high altitude operation of an aircraft 2-stroke Diesel engine. Energy Convers Manage 2015;101:470-480.

[2] Pohorelsky L, Brynych P, Macek J. Air System Conception for a Downsized Two-Stroke Diesel Engine. SAE Paper 2012-01-0831; 2012.

[3] Chen J, Zhuge W, Zheng X, Zhang Y. Investigation of influence of two-stage turbocharging system on engine performance using a pre-design model. In: Proceedings of ASME Turbo Expo 2013: turbine technical conference and exposition GT2013, San Antonio, Texas, USA; June 3-7, 2013.

[4] Ravi M, Marathe A. Effect of Port Sizes and Timings on the Scavenging Characteristics of a Uniflow Scavenged Engine. SAE Paper 920782; 1992.

[5] Ravi M, Marathe A. Effect of Inlet and Exhaust Pressures on the Scavenging Characteristics of a Carbureted Uniflow Scavenged Engine. SAE Paper 920840; 1992.

[6] Fleck R, Cartwright A. Coefficients of Discharge in High Performance Two-Stroke Engines. SAE Paper 962534; 1996.

[7] Schuh D, Chehroudi B. LDV Measurements of Intake Port Flow in a Two-Stroke Engine with and without Combustion. SAE Paper 920424; 1992.

[8] Ekenberg M, Johansson B. The Effect of Transfer Port Geometry on Scavenge Flow Velocities at High Engine Speed. SAE Paper 960366; 1996.

[9] Kinoshita H, Motoyama Y. The Relationship Between Port Shape and Engine Performance for Two-Stroke Engines. SAE Paper 1999-01-3333; 1999.

[10] Mattarelli E, Cantore G, Rinaldini CA. Advances in Internal Combustion Engines and Fuel Technologies. Intech; 2013

[11] Leep LJ, Strumolo G, Griaznov VL., Sengupta S, Brohmer AM, Meyer J. CFD Investigation of the Scavenging Process in a two stroke Engine. SAE Paper 941929; 1994.

[12] Tamamidis P, Assanis D. Optimization of Inlet Port Design in a Uniflow-Scavenged Engine Using a 3-D Turbulent Flow Code. SAE Paper 931181; 1993.

[13] Jia B, Smallbone A, Zuo Z, Feng H, Roskilly AP. Design and simulation of a two- or four-stroke free-piston engine generator for range extender applications. Energy Convers Manage 2016;111:289-298.

[14] Cantore G, Mattarelli E, Rinaldini CA. A new design concept for 2-Stroke aircraft Diesel engines. Energy Procedia 2014;45:739-748.

[15] Scott Goldsborough S, Van Blarigan P. Optimizing the Scavenging System for a Two-Stroke Cycle, Free Piston Engine for High Efficiency and Low Emissions: A Computational Approach. SAE Paper 2003-01-0001; 2003.

[16] Carlucci AP, De Risi A, Donateo T, Ficarella A. A Combined Optimization Method for Common Rail Diesel Engines. In: Proceedings of 2002 Spring Technical Conference of the ASME Internal Combustion Engine Division, Rockford (Illinois, USA); April 14-17, 2002.

[17] Avl BOOST, Users Guide for AVL BOOST - AVL List GmbH, 2008.

[18] Blair GP. Design and Simulation of Two-Stroke Engines. SAE International, Warrendale, 1996.

[19] ModeFrontier User's Manual. ESTECO, 2011.

[20] Ferguson CJ. An Effect Size Primer: A Guide for Clinicians and Researchers. Prof Psychol Res Pr 2009; 40(5): 532-538.

[21] Cohen J. Statistical power analysis. Curr Dir Psychol Sci 1992; 1(3): 98-101.

[22] Cohen J. A power primer. Psychological Bulletin 1992; 112(1): 155-159.

9. Abbreviations

A	Area of the single scavenging port
AFR	Air/fuel ratio
ATDC	After top dead center
BDC	Bottom dead center
BSFC	Brake specific fuel consumption
CAD	Crank angle degree
CC	Cruise condition
CR	Engine volumetric compression ratio
DoE	Design of experiment
DR	Delivery ratio
ES	Effect size
EVC	Exhaust valves closing
EVO	Exhaust valves opening

HBI	Distance between bottom edge of the scavenging ports and bottom dead center
HEV	Exhaust maximum valve lift
HP	High pressure
IPO	Inlet/scavenging ports opening angle
LP	Low pressure
n	Number of inlet/scavenging ports
P_b	Engine brake power
PR_{HP}	High pressure compressor pressure ratios
PR_{LP}	Low pressure compressor pressure ratios
S	Significance
SE	Scavenging efficiency
SL	Sea level
TE	Trapping efficiency

List of Figure captions

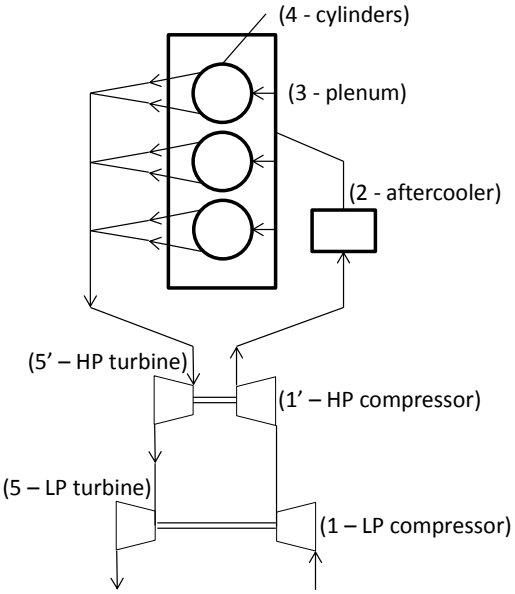
(4 - cylinders)
(3 - plenum)
(2 - aftercooler)
(5’ – HP turbine)
(1’ – HP compressor)
(5 – LP turbine)
(1 – LP compressor)

Figure 1

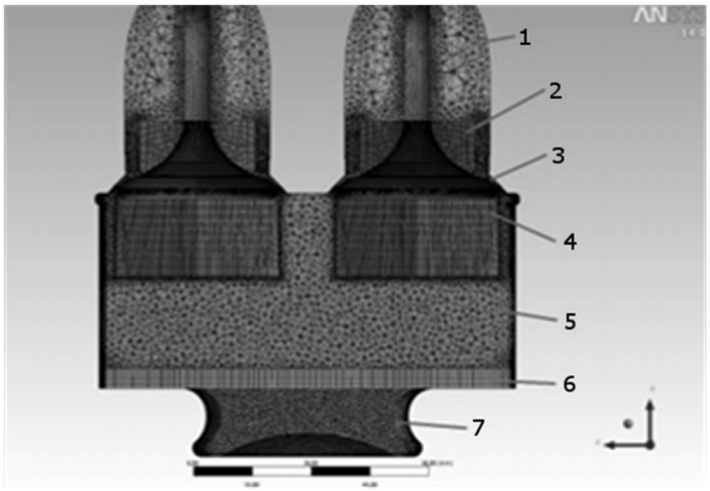

Table 1 - Mesh Zone Overview

ID	Zone	Mesh Motion
1	Outlet	Fixed
2	Part a	Layering
3	Part b	Layering
4	Part c	Layering
5	Cham-zone	Fixed
6	Cyl-zone	Layering
7	Bowl-zone	Rigid Body

Figure 2

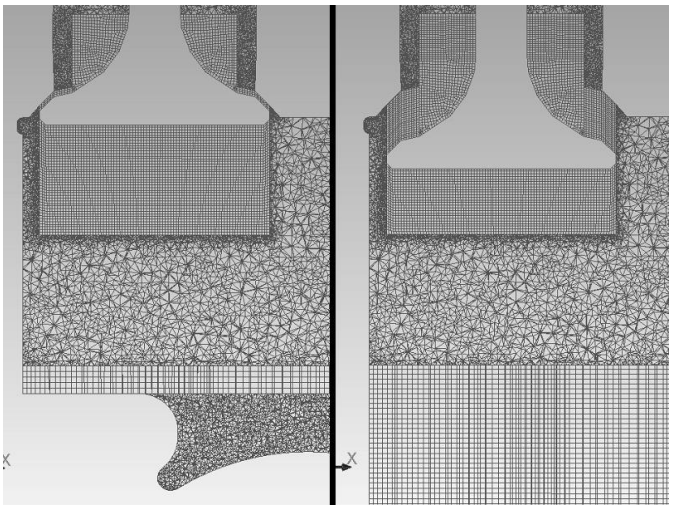

Figure 3

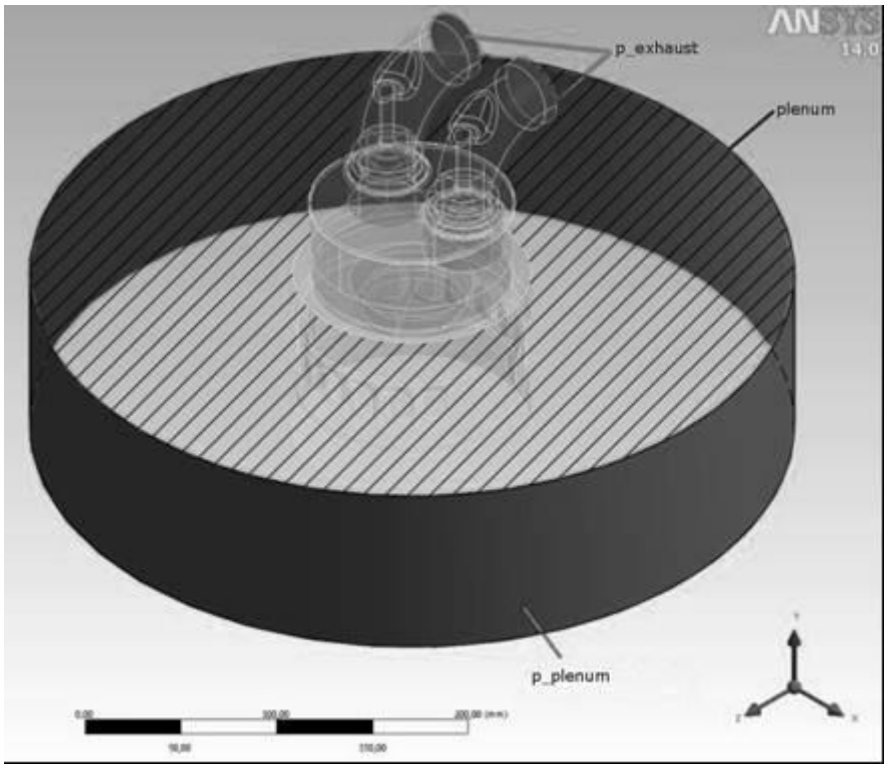

Figure 4

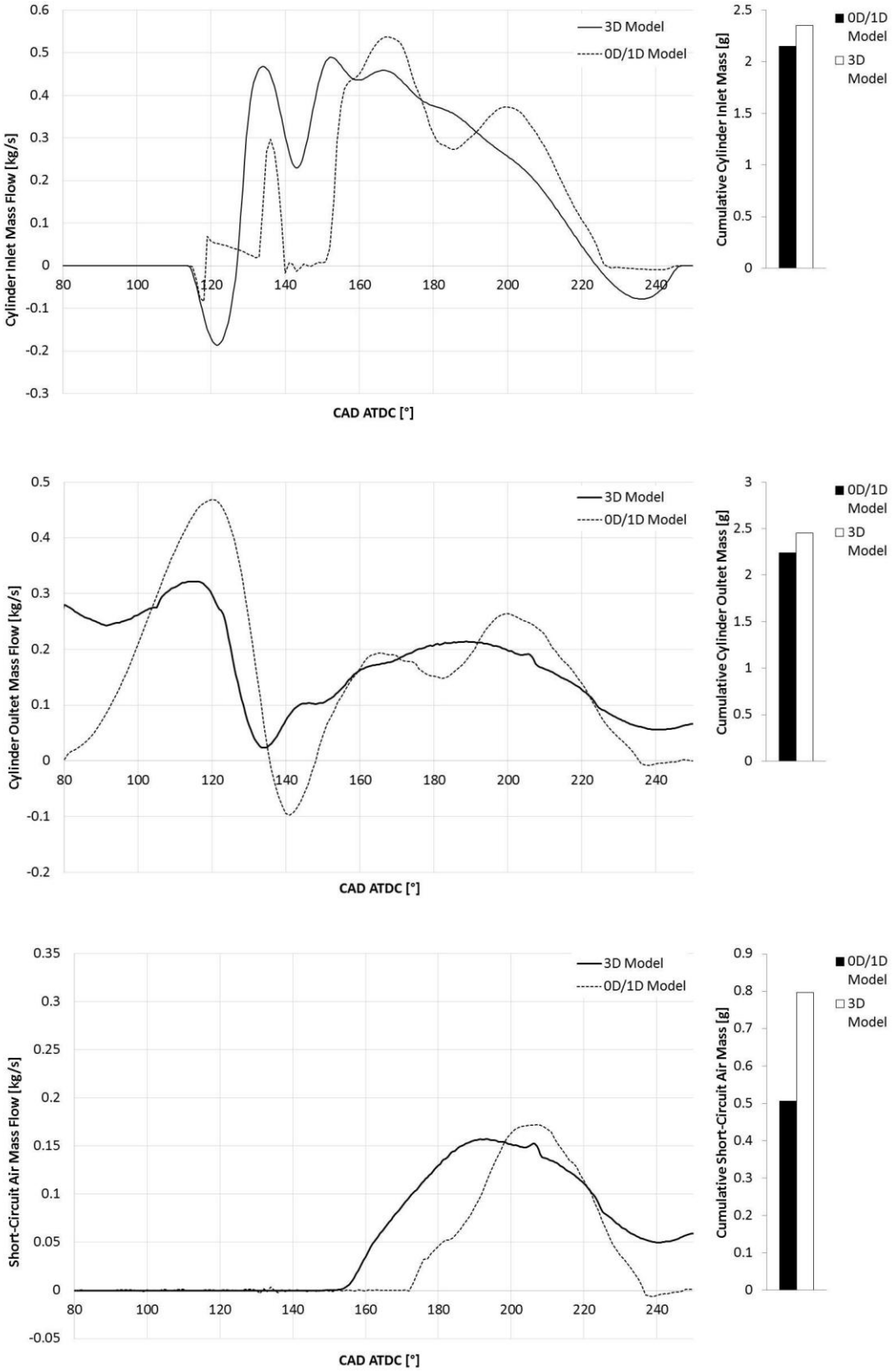
Cylinder Inlet Mass Flow [kg/s]
CAD ATDC [°]
3D Model
0D/1D Model
Cumulative Cylinder Inlet Mass [g]
0D/1D Model
3D Model
Cylinder Oultet Mass Flow [kg/s]
CAD ATDC [°]
3D Model
0D/1D Model
Cumulative Cylinder Oultet Mass [g]
0D/1D Model
3D Model
Short-Circuit Air Mass Flow [kg/s]
CAD ATDC [°]
3D Model
0D/1D Model
Cumulative Short-Circuit Air Mass [g]
0D/1D Model
3D Model

Figure 5

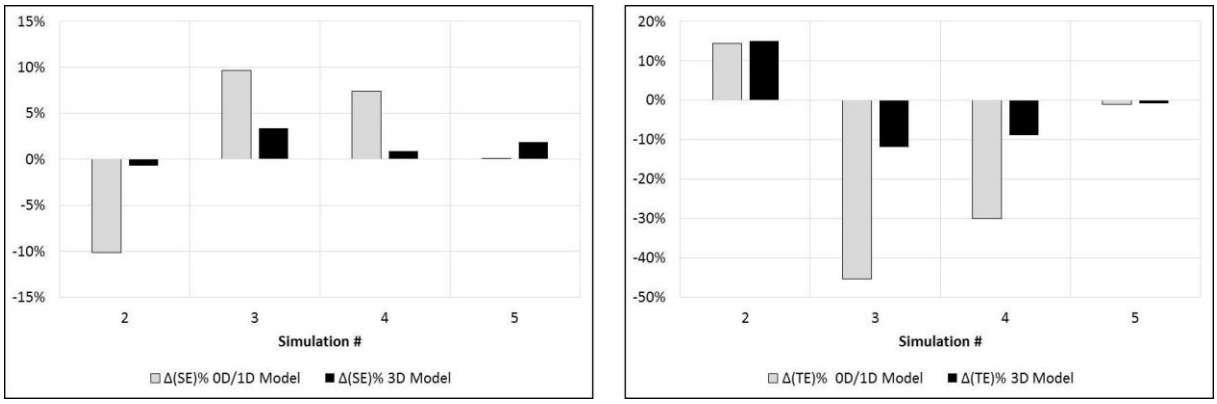
15%
10%
5%
0%
-5%
-10%
-15%
2
3
4
5
Simulation #
Δ(SE)% 0D/1D Model
Δ(SE)% 3D Model
20%
10%
0%
-10%
-20%
-30%
-40%
-50%
2
3
4
5
Simulation #
Δ(TE)% 0D/1D Model
Δ(TE)% 3D Model

Figure 6

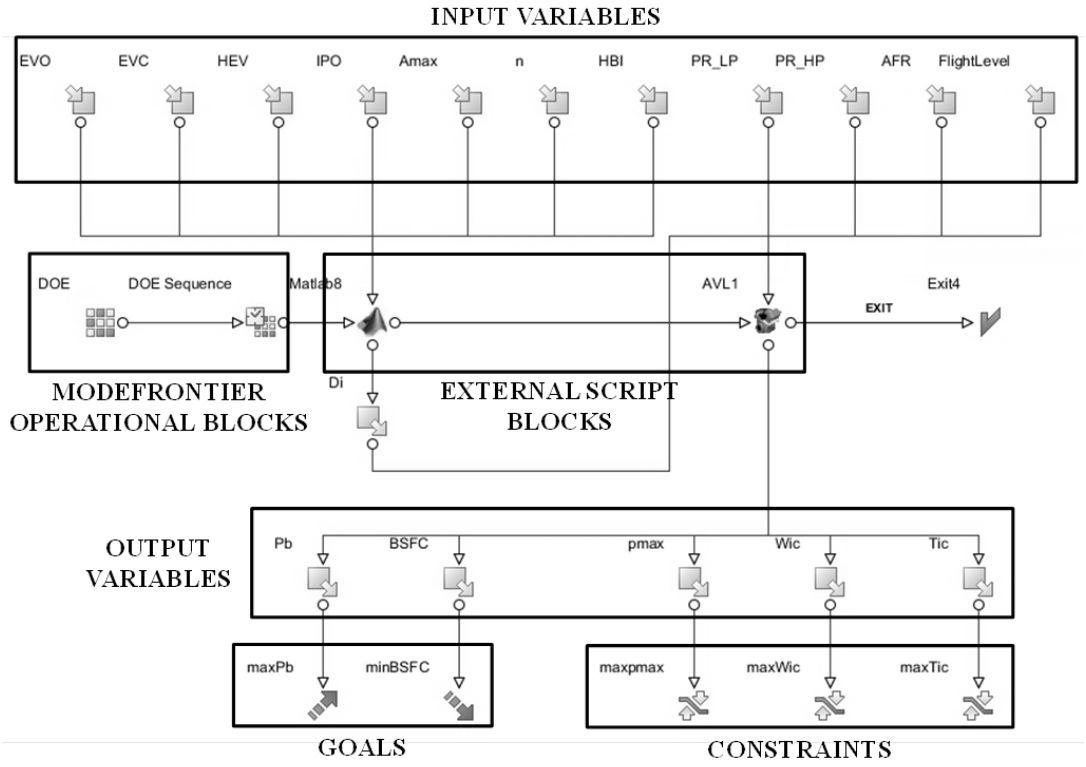
INPUT VARIABLES
EVO
EVC
HEV
IPO
Amax
n
HBI
PR_LP
PR_HP
AFR
FlightLevel
DOE
DOE Sequence
Matlab8
AVL1
Exit4
EXIT
Di
MODEFRONTIER
OPERATIONAL BLOCKS
EXTERNAL SCRIPT
BLOCKS
OUTPUT
VARIABLES
Pb
BSFC
pmax
Wic
Tic
maxPb
minBSFC
maxpmax
maxWic
maxTic
GOALS
CONSTRAINTS

Figure 7

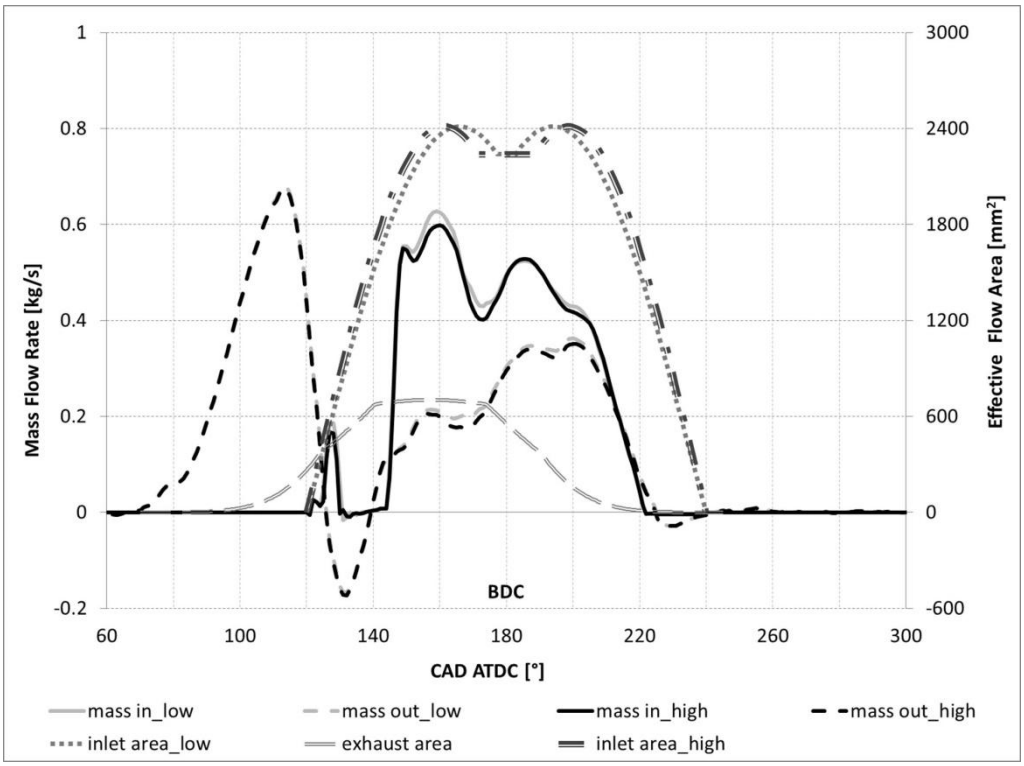
1
0.8
0.6
0.4
0.2
0
-0.2
3000
2400
1800
1200
600
0
-600
Mass Flow Rate [kg/s]
Effective Flow Area [mm²]
BDC
60
100
140
180
220
260
300
CAD ATDC [°]
mass in_low
mass out_low
mass in_high
mass out_high
inlet area_low
exhaust area
inlet area_high

Figure 8

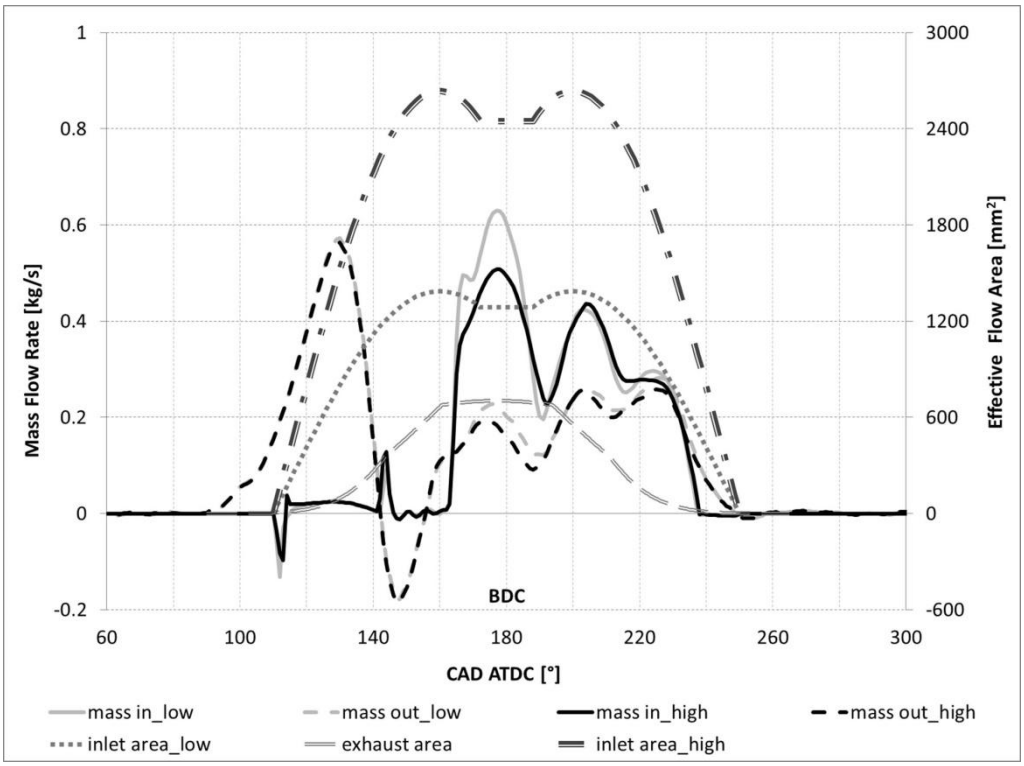
1
0.8
0.6
0.4
0.2
0
-0.2
3000
2400
1800
1200
600
0
-600
Mass Flow Rate [kg/s]
Effective Flow Area [mm²]
BDC
60
100
140
180
220
260
300
CAD ATDC [°]
mass in_low
mass out_low
mass in_high
mass out_high
inlet area_low
exhaust area
inlet area_high

Figure 9

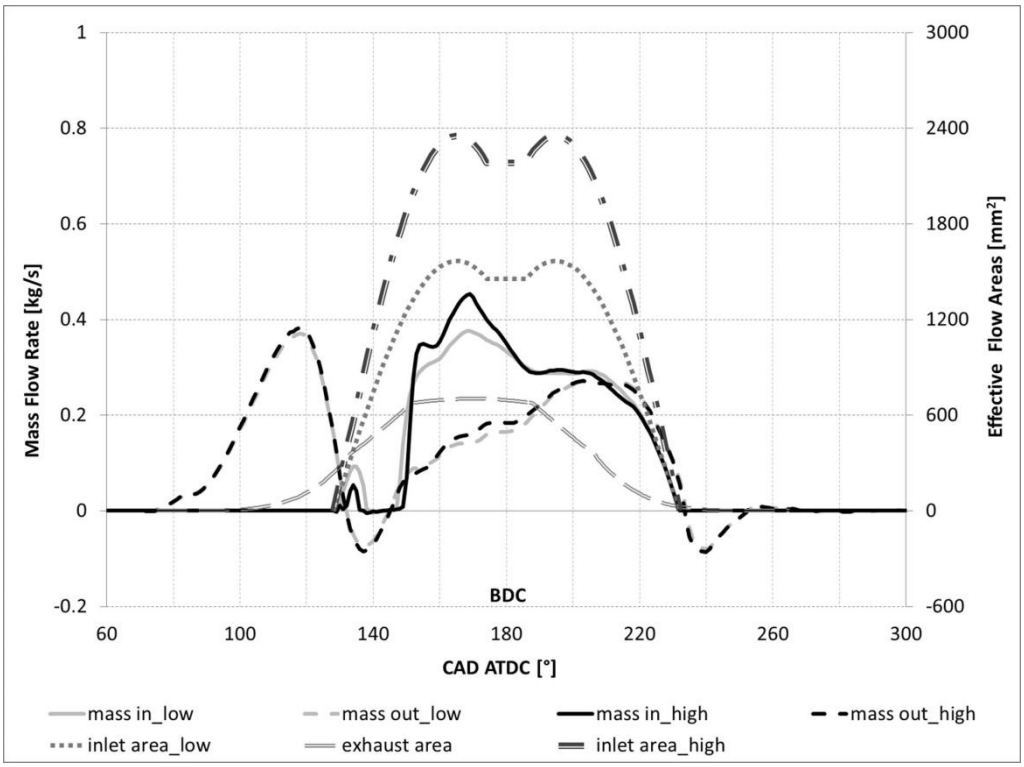
1
0.8
0.6
0.4
0.2
0
-0.2
Mass Flow Rate [kg/s]
3000
2400
1800
1200
600
0
-600
Effective Flow Areas [mm²]
BDC
60
100
140
180
220
260
300
CAD ATDC [°]
mass in_low
mass out_low
mass in_high
mass out_high
inlet area_low
exhaust area
inlet area_high

Figure 10

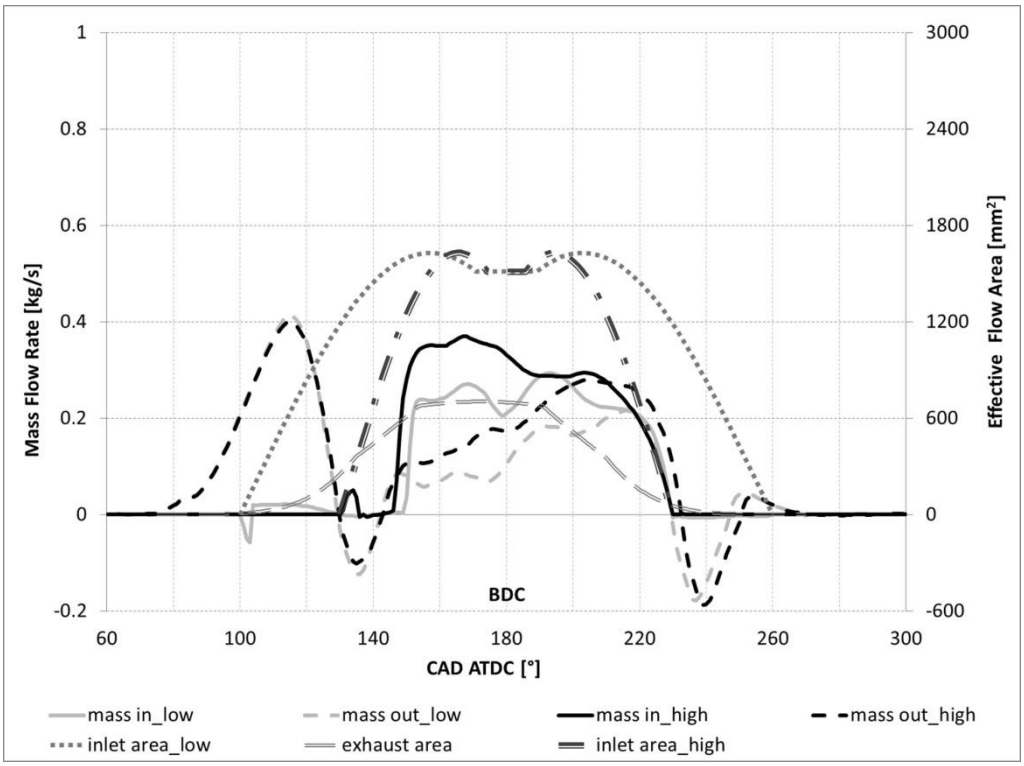
1
0.8
0.6
0.4
0.2
0
-0.2
3000
2400
1800
1200
600
0
-600
Mass Flow Rate [kg/s]
Effective Flow Area [mm²]
BDC
60
100
140
180
220
260
300
CAD ATDC [°]
mass in_low
mass out_low
mass in_high
mass out_high
inlet area_low
exhaust area
inlet area_high

Figure 11

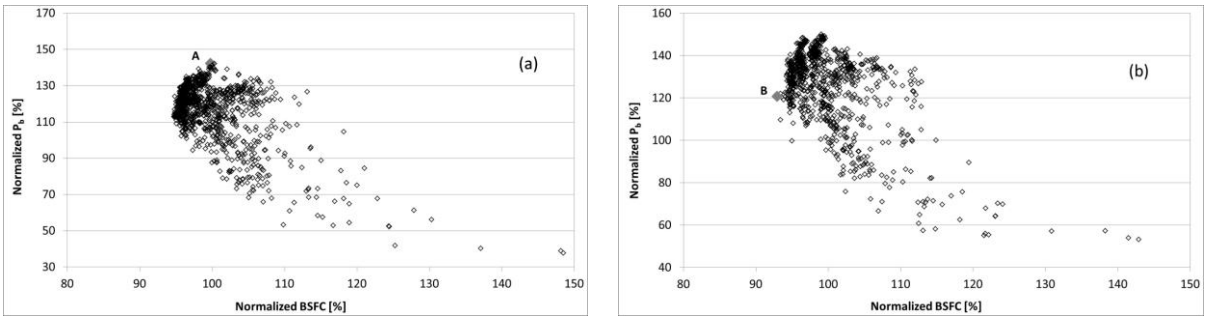
(a)
A
Normalized P_k [%]
Normalized BSFC [%]
(b)
B
Normalized P_k [%]
Normalized BSFC [%]

Figure 12